

Large-Eddy Simulation and Control of Cavity Aeroacoustics

H. Lai and K. H. Luo

School of Engineering Sciences, University of Southampton,
Highfield, Southampton SO17 1BJ, U.K.

ABSTRACT

In the present study, a sound control technique for a three-dimensional open cavity flow was explored using LES combined with the Ffowcs Williams-Hawkings acoustic analogy. Porous media were inserted on the cavity floor or rear wall, and the effect of the porous media was modelled using the Darcy pressure - velocity law. Consequently, flow in the cavity could move in or out through the porous walls, depending on the local pressure difference. Large-eddy simulations were carried out for the near field, and acoustic analogy was used to predict sound radiation. The study showed that applying porous media on cavity floor or rear wall could effectively decrease the sound pressure level. The modes of flow oscillations in the cavity remained largely the same, although the dominant oscillation frequencies were changed. As a result, the dominant sound source term induced by the transverse fluctuations was reduced. The study also showed the sound radiation from the present realistic cavity geometry followed the pattern of three-dimensional wave propagation, and the sound pressure in the far-field was suppressed by using porous walls in the cavity.

INTRODUCTION

Compressible flow over cavities involves non-linear interactions among shear layer instabilities, turbulence, structure and aeroacoustics. The time and length scales of these phenomena are widely disparate, which presents severe challenges for theoretical, numerical and experimental studies. Recently, direct numerical simulation (DNS) and large-eddy simulation (LES) have been applied successfully to cavity flow and associated aeroacoustic problems [1, 2, 3], which has contributed to enhanced understanding of the complex interactions and the sound generation mechanisms.

However, control of aeroacoustics generated by cavity flow is still an unsolved problem. Over the past few decades, there have been various passive, active and reactive (anti-sound) control techniques developed for sound reduction in general, reviewed in [4], for example. These control techniques include installing a spoiler or vortex generator near the separation point, modifying the geometry of the leading or the trailing edge (ramps), placing small rods in crossflow just upstream of the cavity, using passive “resonance tubes” and slotted, vented or slanted cavity walls, to name just a few. A varying degree of success has been achieved, but most techniques would dramatically change the original flow, leading to some undesirable effects.

In the present study a different sound control technique was explored using LES coupled with the Ffowcs Williams-Hawkings (FW-H) acoustic analogy. A schematic of the strategy is illustrated in Figure 1. Basically, porous media were used for the cavity floor and/or rear wall instead of the usual solid walls. Consequently, flow in the cavity could move in or out through the porous walls, depending on the local pressure

difference in the cavity flow and in the porous media. As a result, highly unsteady flow in the cavity may become modulated and strength of vortices may reduce, leading to reduced sound emission.

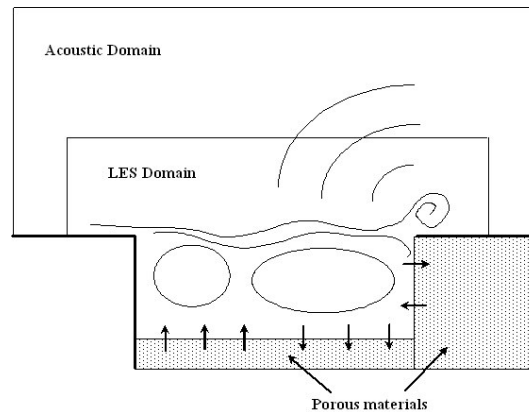


Figure 1: Flow configuration of the cavity with porous walls.

HYBRID LES-AOUSTIC ANALOGY APPROACH

The basic methodology of the LES-acoustic analogy was described in [3], which in this study was extended to simulate the interaction between the cavity flow and the porous cavity walls in this study.

LES and numerical method

The non-dimensional Favre-filtered Navier-Stokes and energy equations for unsteady compressible flow are solved, supplemented by subgrid-scale (SGS) models. In order to focus on the integration of an LES solver with an acoustic solver, the standard Smagorinsky eddy-viscosity model is employed in the momentum equations. The filtered energy equation contains at least six unknown SGS terms, the modelling of which is not yet established.

Here we adopt the simplified treatment of Larcheveque et al. [5]. As the Smagorinsky model does not have a proper behaviour as solid walls are approached, the length scale in the model is corrected by the Van Driest damping function: $l = Cs\Delta[1 - \exp(-y^+/25)]^{0.5}$, where Cs is a constant set to 0.17, Δ the filter width and y^+ the normalised distance to the wall.

The LES code used was previously designed for simulating shock/boundary-layer interaction (SBLI) [6]. An entropy-splitting approach is employed, which improves the non-linear stability and minimizes numerical dissipation. The finite difference scheme has fourth-order accuracy in spatial discretization and a third-order temporal resolution. The code uses multi-block meshes and can handle complex geometries. It is parallelised using the MPI algorithm and optimized for parallel computers.

The 3D cavity configuration studied includes cavity side walls, with a length-to-depth ratio $L/D = 5$, width-to-depth ratio $W/D = 1$. The computational mesh consists of the cavity block (BL1) and the block outside cavity (BL2). The upstream and downstream boundaries are located at $4D$ from the leading and trailing edges of the cavity, respectively. The upper horizontal boundary is set at $7D$ so that the computational domain includes a portion of the acoustic field. The spanwise length of BL2 is set as $W_2 = 2W$. The grid points in x - y - z directions are $151 \times 61 \times 61$ in BL1 and $301 \times 121 \times 121$ in BL2. Non-reflecting boundary conditions are applied at the inflow, top and outflow boundaries. On solid walls, an isothermal wall condition is prescribed and a no-slip condition is imposed on velocity components. At the inflow, the mean velocity is specified using a power law. Small disturbances with magnitudes up to 4% of the mean streamwise velocity are added at the inflow boundary.

Modelling of porous material

In order to model the effect of using porous media as cavity walls, a constant back pressure is maintained inside the porous zones [7]. According to the linear form of the Darcy pressure-velocity law, this gives

$$v_w = \sigma(p_i - p_w) / \rho_\infty u_\infty, \quad (1)$$

where v_w and p_w are the normal velocity and the pressure on the porous surface, σ the geometric porosity and p_i the back pressure. This constant back pressure is equivalent to a chamber behind a porous wall. In the LES, the pressure was set to be the average of the pressure along the walls, so that there was no net mass influx or outflux across the flow-wall interface in a statistical sense.

Acoustic analogy

Ffowcs Williams and Hawkings [8] obtained a most general form of the Lighthill analogy by incorporating arbitrary motion of aerodynamic surfaces. In the FW-H formulation, the integration surface can be permeable, allowing mass, momentum and energy to pass through it. This feature offers a high degree of flexibility in positioning the integration surface, which is of great practical importance. For the current cavity flow, solution of the FW-H equation was obtained using the three-

dimensional frequency/space Green function method as following [2, 3]:

$$p'(\bar{x}, \omega) = \int_{f=0} F_i(\bar{y}, \omega) \frac{\partial G(\bar{x}|\bar{y}, \omega)}{\partial y_i} d\Sigma + \int_{f=0} i\omega Q(\bar{y}, \omega) G(\bar{x}|\bar{y}, \omega) d\Sigma \quad (2)$$

where p' is the Fourier transform of the sound pressure p' . $f = 0$ defines the integration surface Σ , which separates the sound source region ($f < 0$) from the acoustic field ($f > 0$). The free-space Green function is

$$G(\bar{x}|\bar{y}, \omega) = -\exp\left(i \frac{k}{\beta^2} [r_\beta - M_\infty(x_1 - y_1)]\right) / 4\pi r_\beta,$$

where

$$\beta = \sqrt{1 - M^2} \quad (M < 1),$$

$$r_\beta = \sqrt{(x_1 - y_1)^2 + \beta^2(x_2 - y_2)^2 + \beta^2(x_3 - y_3)^2}.$$

\bar{x} is the observer position and \bar{y} denotes a source point. The barred variables Q and F_i are the Fourier transform of the terms in the monopole and dipole sound sources:

$$Q = (\rho u_i - \rho_\infty U_i) \partial f / \partial x_j,$$

$$F_i = -[\rho(u_i - 2U_i)u_j + p\delta_{ij} + \rho_\infty U_i U_j - \tilde{\sigma}_{ij}] \partial f / \partial x_j.$$

U_i is the velocity component of the uniform background flow; (t, x_i) are the temporal and spatial coordinates in the observer flow domain; The viscous stress $\tilde{\sigma}_{ij}$ is generally negligible. The position and the shape of the integration surface $f=0$ are not necessarily fixed. This provides flexibility for placing the integral surface so that the quadrupole sources can be enclosed in the integral surface and omitted, which greatly simplifies the calculation.

In the current study, the integration surface is a plane placed horizontally at a distance of $s=D$ above the cavity. During LES, a time series of F_i and Q are recorded and transformed into the frequency domain, using discrete Fourier transformation (DFT) to obtain F_i and Q . The sound pressure in the frequency domain is then calculated using Eq. (2). Finally, an inverse discrete Fourier transformation is carried out to obtain the instantaneous sound pressure at the observer position \bar{x} .

RESULTS

The cavity configuration with all solid walls was used in a series of experimental measurements in the UK's DSTL. The LES simulations correspond to the experimental case M219, which had an inflow Mach number 0.85 and a Reynolds number $Re_D = 1.36 \times 10^6$ [9]. Two additional cases with porous cavity floor (Case B) and porous rear wall (Case C), respectively, are simulated, and compared with the original cavity case with solid walls (Case A). For all the three cases, the LES simulations start from the same uniform initial field. Time marching is based on a CFL number of unity which corresponds to a non-dimensional time step of about 2.5×10^{-4} . The flow enters a self-sustained oscillation state after an initial transient stage of about 15 to 20 non-dimensional time units but the simulation is carried on for a period of 5 flow-throughs for the development of the flow field. Then the sound monopole Q and dipole F_i for FW-H are recorded for a time

period of $\Delta t_2 = 7.46$, which approximately equals to the period of the second Rossiter mode. This sampling period for the sound sources may be not long enough to include all the oscillation modes, but it is believed that the main sources of sound are included. The use of the Smagorinsky SGS model may also affect the results, due to its well known defects. However, relatively high grid resolution was employed in the present simulations, so the effects of the SGS model should be small. Moreover, the main sound sources are mostly associated low-frequency, large-scale structures, which the Smagorinsky model can predict reasonably well.

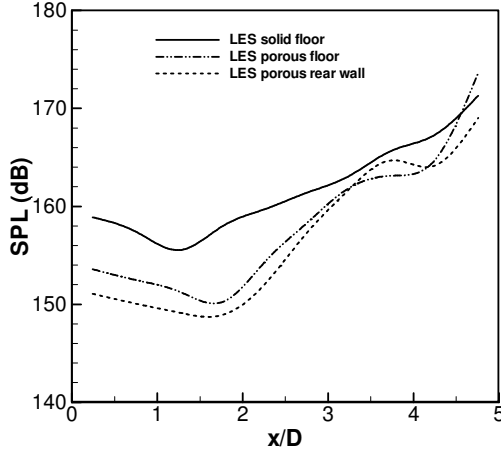


Figure 2: Comparison of SPL along the cavity floor.

Figure 2 shows the sound pressure level (SPL) at a series of monitoring points on the cavity floor along the line $z/D = 0.625$. The SPL is defined as:

$$\text{SPL (dB)} = 20 \log_{10}(p'_{rms}/2 \times 10^{-5} \text{ Pa}), \quad (3)$$

where p'_{rms} is the root-mean-square sound pressure. Comparison of the result of Case A (with all solid walls) with experimental data has been provided in our previous work [3], where reasonably good agreement was obtained. As there are no experimental data for the porous cases, the present paper will focus on parametric studies only. When the cavity floor or rear wall is changed into porous media, the SPL on the cavity floor are effectively reduced. The porous rear wall case seems to be slightly more effective in sound reduction than the other case. This is because flow impingement on the rear wall is a major source of sound. The porous rear wall reduces the impact of the impingement, helping to reduce flow deflection and wave reflection from the rear wall.

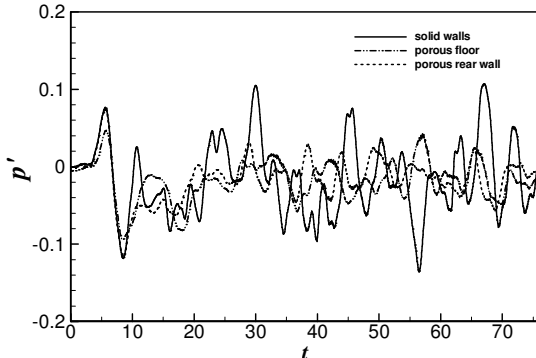


Figure 3: Monitored pressure oscillations on cavity floor at $(x, y, z)=(2.75D, 0, 0.625D)$.

Figure 3 shows the pressure oscillation at a monitoring point on the floor at $(x, y, z) = (2.75D, 0, 0.625D)$. The amplitude of the oscillation is suppressed when porous media are used. The pressure spectrum shown in Figure 4 demonstrates that the use of porous media does not change the pressure oscillation pattern significantly. However, changes in oscillating frequencies are observed. The amplitudes of dominant Rossiter modes, which are major sources of sound, are reduced by applying the porous media.

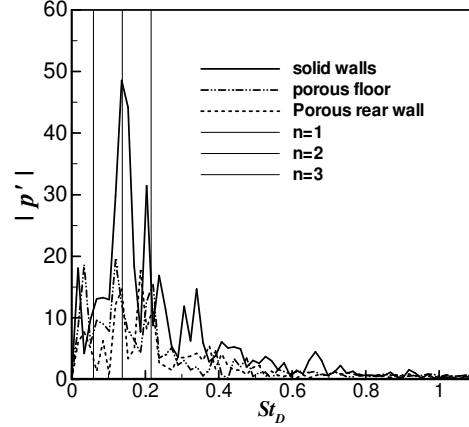


Figure 4: Spectrum of pressure oscillation at the monitoring point on the cavity floor at $(x, y, z) = (2.75D, 0, 0.625D)$.

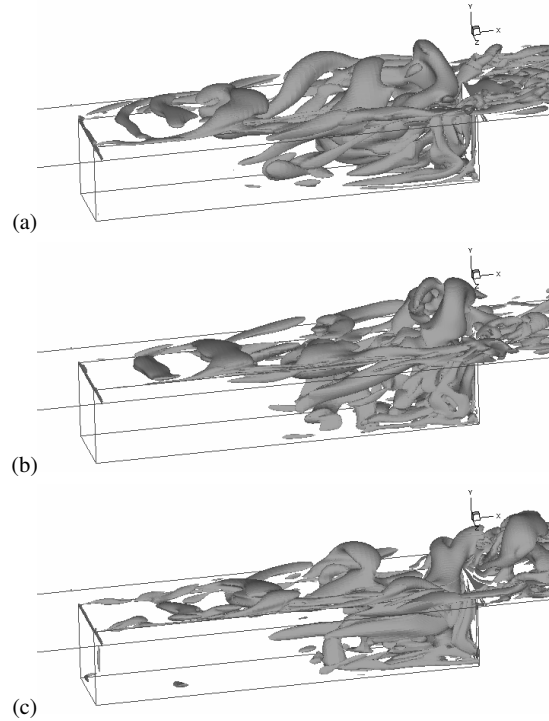


Figure 5: Comparison of instantaneous vortical structures at $t=76$, (a) all solid walls, (b) porous cavity floor, and (c) porous cavity rear wall.

Figure 5 compares the snap shots of the 3D vortical structures at an arbitrary instant for three cases. Quite complex and unsteady vortex structures are featured. Large spanwise vortices are generated periodically near the cavity leading edge. These vortices are spanwise

rollers extending to the two side walls at the beginning but quickly become bended in the spanwise direction, so that longitudinal structures start to appear at the roller's two ends. The zone in which spanwise vortical structures dominate is much shorter than that seen typically in 2D simulations. Shortly downstream, the large vortices break up into smaller vortices, which are irregular and highly 3D. The vortical structures are especially complex near the cavity rear wall, due to flow impingement and recirculation. Comparison of the three cases shows that the large-scale structures or flow oscillation patterns with or without the porous walls are quite similar, although the oscillation phase may be slightly different.

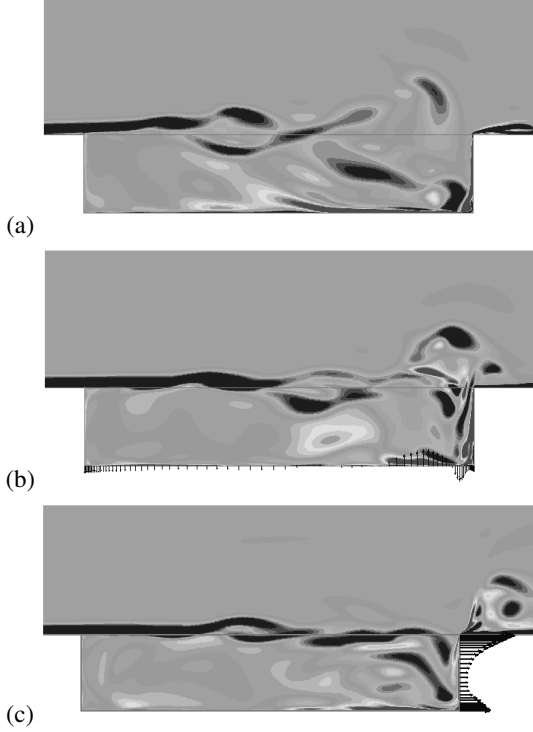


Figure 6: Comparison of instantaneous flow pattern at $t=76$ in the geometrical centre plane of the cavity, (a) all solid walls, (b) porous cavity floor, and (c) porous cavity rear wall. The greyscales are the spanwise vorticity, with values from -2 to 2, at 15 levels. The velocity vectors on the floor are shown at one in every 3 points.

Figure 6 shows the instantaneous flow patterns in the cavity and the associated flow through the porous walls. The periodical oscillation of the shear layer produces pressure wave moving in the cavity, travelling and reflecting between the front and rear walls according to the Rossiter loop. The pressure difference between the cavity walls and p_i in the porous media results in near-wall flow into or out of the porous media. The pressure oscillation on the cavity floor is modulated and the SPL is lowered.

The change of flow in the cavity by the use of porous media also introduces changes in the sound sources and consequently the sound radiation into the far-field. The variation of F_i ($i=1, 2$ and 3 for the x -, y - and z -directions, *i.e.*, the streamwise, transverse and spanwise directions, respectively) and Q are analysed. Our results show that

the y - direction term F_2 has higher order magnitude than the x - and z - components and the monopole term Q . This indicates that sound radiation is mostly due to the flow fluctuations in the y - direction. The variation of F_2 during a non-dimensional time duration of $dt = 7.3$, corresponding to the period of the second Rossiter mode, is shown in Figure 7. Clearly, the porous floor and porous rear wall cases have smaller F_2 values than that of the original solid-wall case.

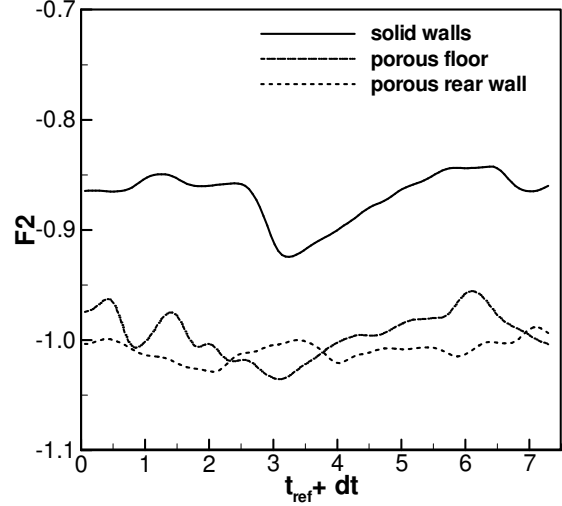


Figure 7: Comparison of F_2 associated with the dipole source during a time period corresponding to the second Rossiter mode. $t_{ref}=60$ is the starting time of recording the sound source in all the three LES cases.

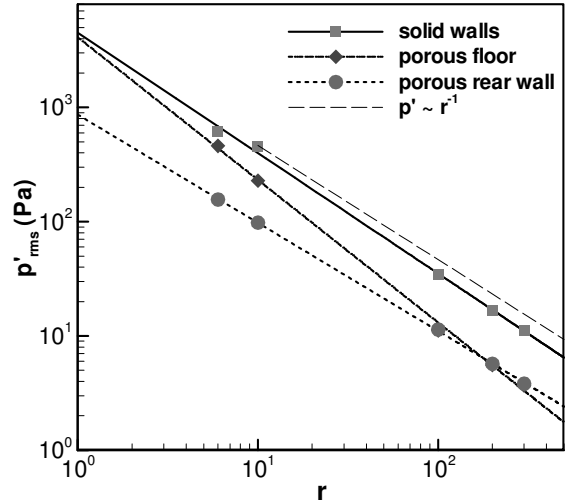


Figure 8: Decaying of sound pressure p'_{rms} with the increase in r at $\theta=60^\circ$ in the cavity center plane. r is the distance of an observer from the cavity mouth centre, θ is the radial angle, measured from the downstream top plane of the cavity.

Figure 8 compares the damping of the sound pressure p'_{rms} with the distance away from the cavity, r . According to the linear acoustics theory, sound pressure from a single point source decays following the spherical damping law of $p' \sim r^{-1}$, which is also shown in the figure together with the present predictions. It is shown that for the three cases studied in this paper, we have $p' \sim r^\alpha$, where the parameter α varies slightly around the value -1. For the solid case,

$\alpha \approx 1$. In other cases, α is modified. It suggests that the use of porous cavity wall has a damping effect on the far-field sound, so that the linear acoustic theory is no longer adequate.

CONCLUSIONS

A sound control technique using porous walls for a three-dimensional cavity flow was explored using LES and the Ffowcs Williams-Hawkings acoustic analogy. Porous media are used as the floor or the rear wall of the cavity and modelled using the Darcy pressure - velocity law. Large-eddy simulations are carried out for the near field, and acoustic analogy is used to predict sound radiation. Applying the porous surfaces allows flow in the cavity to move in or out of the porous walls, depending on the local pressure difference between the cavity flow field and the porous media. The study shows that the use of porous media as cavity walls can modulate the cavity flow and effectively decrease the sound pressure level. Changes of the frequencies of the dominant oscillation modes are observed but the mechanisms of flow oscillation remain largely the same. The dominant sound source term is related to the transverse flow fluctuations, which is reduced by the use of porous walls. In the far-field, sound radiation from the cavity for the three cases is shown to follow the three-dimensional wave propagation pattern. Modulation of the sound source field by using porous cavity walls has a damping effect on the far-field sound level, which invalidates the linear acoustic propagation theory.

ACKNOWLEDGEMENTS

The work was funded by the UK EPSRC and MOD/DSTL under Grant No. GR/R85303/01. Thanks are due to Dr. Trevor Birch and Dr. Graham Foster at DSTL for their support and collaboration. The computing resources were from the UK Turbulence Consortium under the EPSRC Grant No. GR/R64964/01.

REFERENCES

- [1] Larchevêque L., Sagaut P., Lê T. and Comte P. “*Large-Eddy Simulation of a Compressible Flow in a Three-Dimensional Open Cavity at High Reynolds Number*” Journal of Fluid Mechanics, Vol. 516, pp. 265-301, 2004-12-06.
- [2] Gloerfelt X., Bailly C. and Juve D. “*Direct computation of the noise radiated by a subsonic cavity flow and application of integral methods*” Journal of Sound and Vibration, Vol. 266, pp. 119-146, 2003.
- [3] Luo K.H. and Lai H. “*A hybrid LES-acoustic analogy method for computational aeroacoustics*” The 6th ERCOFTAC Workshop on Direct and Large-Eddy Simulation, Poitiers, France, September 12-14, 2005.
- [4] Colonius, T. “*An overview on simulation, modelling, and active control of flow/acoustic resonance in open cavities*”, AIAA paper 2001-0076.

[5] Larcheveque L., Sagaut P., Mary I., Labbe O. and Comte P. “*Large-eddy simulation of a compressible flow past a deep cavity*” Physics of Fluids, Vol. 15, No. 1, pp. 193-210, 2003.

[6] Sandham N. D., Yao Y. F. and Lawal A. A. “*Large-eddy simulation of transonic turbulent flow over a bump*” International Journal of Heat and Fluid Flow, Vol. 24, pp.584-595, 2003.

[7] Kim I. and Chokani N. “*Navier-Stokes study of supersonic cavity flowfield with passive control*”, Journal of Aircraft, Vol. 29, No.2, pp. 217-223, 1992.

[8] Ffowcs Williams J. E. and Hawkings D. L. “*Sound generated by turbulence and surfaces in arbitrary motion*” Philosophical Transactions of the Royal Society, A, Vol. 264 (1151), pp. 321-342, 1969.

[9] De M. J. and Henshaw C. “*M219 cavity case. In Verification and Validation Data for Computational Unsteady Aerodynamics*” Tech. Rep. RTO-TR-26, AC/323(AVT)TP/19, pp. 453-472, 2000.